Accurate Temperature Measurements for Medical Research using Body Sensor Networks

Carlo Alberto Boano*, Matteo Lasagni*‡, Kay Römer*, and Tanja Lange†

*Institute of Computer Engineering
University of Lübeck
Lübeck, Germany
{cboano, roemer}@iti.uni-luebeck.de

‡Dip. di Scienze e Metodi dell'Ingegneria
University of Modena and Reggio Emilia
Reggio Emilia, Italy
matteo.lasagni@unimore.it

†Department of Neuroendocrinology
University of Lübeck
Lübeck, Germany
lange@kfg.uni-luebeck.de

***Abstract*—Medical measurements and clinical trials are often carried out in controlled lab settings – severely limiting the realism and duration of such studies. Our goal is henceforth to design a body sensor network for unobtrusive and highly-accurate profiling of body parameters over weeks in realistic environments. One example application is monitoring the impact of sleep deprivation on periodic processes in the human body known as circadian rhythms, which requires highly-accurate profiling of skin temperature across the human body over weeks with real-time feedback to a remote medic.**

We analyze the requirements on a body sensor network for such applications and highlight the need for self-organizing behavior such as adaptive sampling to ensure energy efficiency and thus longevity, adaptive communication strategies, self-testing, automatic compensation for environmental conditions, or automatic recording of a diary of activities.

As a first step towards this goal, we design and build a prototype of such a non-invasive wearable wireless monitoring system for accurate body temperature measurements and real-time feedback to the medic. Through the design, parameterization, and calibration of an active measurement subsystem, we obtain an accuracy of 0.02°C over the typical body temperature range of 16-42°C. We report results from two preliminary trials regarding the impact of circadian rhythms and mental activity on skin temperature, indicating that our tool could indeed become a valuable asset for medical research[1].

I. Introduction

Wearable Body Sensor Networks (BSN) are a promising emerging technology for unobtrusive real-time monitoring of vital parameters. Their flexibility, low-cost, and uninterrupted operation make them suitable for applications ranging from telemedicine and health care (enhanced diagnostic tools, monitoring of elderly patients and chronic diseases), over e-fitness (monitoring of sporting activities and physical performance) and interactive gaming, to emotion-based applications.

[1]This is the author's version of the work, and it is not meant for redistribution. The definitive version was published in:
SORT'11, March 28-31, 2011, Newport Beach, California.

Body sensor networks have also the potential to revolutionize medical research. A well-known issue in this field is the lack of realism in measurements, also known as "White Coat Syndrome." Patients being visited and monitored in hospital environments often do not behave as in their daily life, due to the stress and anxiety associated with the clinical visit and due to the exposure to a different environment. Unobtrusive 24/7 pervasive monitoring in supportive home environments using miniaturized body sensors would more accurately reflect the true values for a given parameter, therefore improving the accuracy of data available to researchers.

An example of such applications is accurate measurement of body temperature in a continuous fashion. There are many branches of medical science that would benefit from a non-invasive low-cost tool enabling long-term and accurate measurement of body temperature. Psychophysiologists can use peripheral responses, such as variations of skin temperature, as indicators of brain activity, state of mind, or psychological state. Chronobiologists can derive from long-term temperature measurements an accurate profile of the circadian-system activity. The circadian system adjusts and regulates the body's internal organization over the 24-hour day, which is essential to guarantee correct function of, e.g., the central nervous and immune system. Body core and skin temperature follow strong rhythms over the 24-hour day – the so called circadian rhythms. Therefore it is very important to have precise knowledge and understanding of the phase, amplitude, and stability of circadian rhythms, which requires continuous sampling of body temperature over several days. Furthermore, accurate and continuous temperature monitoring can lead to early detection of illness, e.g., breast thermography can indicate early signs of cancer.

In this paper, we design and develop a non-invasive wearable wireless monitoring system for accurate body temperature measurements. Our goal is to support medical research by providing a miniaturized system that collects precise body temperature samples at variable sampling rates ranging from 0.01 to 10 Hz. We use high-precision NTC thermistors, pre-

cision amplifiers, and perform thorough calibration, reaching a temperature accuracy of up to 0.02°C in the temperature range 16-42 °C. The system is designed to be unobtrusively worn by patients in their home environments for several weeks and includes real-time feedback to a care unit, so that the medical staff can continuously monitor the correctness of the collected results and guarantee the health of the patient. We optimize the energy efficiency of our system in order to achieve lifetimes of several weeks at sampling rates in the order of 1 Hz. We validate the correct operation of our system, and show how it can be applied to improve the quality of measurements in medical research.

The paper proceeds as follows: Section II describes several applications of accurate temperature monitoring for medical research, Section III reviews related work in the field. In Section IV we first discuss requirements and then the architecture of our system including the hardware platform we use. Section V describes the integration and calibration of thermistors to achieve high measurement accuracy. We evaluate the obtained accuracy in Section VI, and show the results of two preliminary medical trials. We conclude our paper in Section VII, including an outlook on future work.

II. Applications

In this section we describe our target applications and explain the benefits brought by a continuous ubiquitous temperature monitoring. In particular, we consider the monitoring of circadian rhythms and the study of peripheral responses as indicators of brain activity and emotions.

A. Impact of Sleep Deprivation on Circadian Rhythms

A circadian rhythm is a roughly 24-hours cycle in biological processes such as body temperature, hormone secretion, sleep, and feeding. These rhythms are induced by cellular 'biological clocks' in the brain and in almost all peripheral tissues which are set by exogenous cues – the so called "zeitgebers", like daylight/darkness, waking/sleeping, and feeding/fasting.

Human core body temperature is tightly regulated by the central and peripheral nervous system. Deep and superficial body temperatures are sensed, and in turn heat- and cold-defense responses are regulated (e.g., sweating, shivering, changes in skin blood flow) [1]. Human core body and skin temperature follow strong circadian rhythms over the 24-hour day. In the evening the activity of the sympathetic nervous system – that is one of the major systems in the human body – decreases, and the widening of skin vessels (vasodilatation) in the extremities leads to an increased blood flow to the periphery with a sharp increase in distal skin temperature (i.e., skin temperature at the extremities). An increase in distal skin temperature can also be induced by changes in posture, light, mental activity, hormones, and drugs. In the morning, the changes are reversed: an increase in sympathetic tone induces peripheral vasoconstriction leading to a reduced blood flow to the periphery, as the body redirects the blood flow from the shell to the core (insulation).

The circadian rhythms help to anticipate environmental changes and demands (e.g., low versus high activity of metabolism at night and day, respectively) in order to save energy. Sleepiness and the ability to fall asleep are highest when the distal skin temperature is increasing. In contrast, alertness and performance after awakening are fully restored once the distal skin temperature has newly reached minimum levels. On the one hand, passive warming (e.g., taking a warm bath) can facilitate sleep onset; on the other hand passive cooling (e.g., taking a cold shower) as well as the use of vasoconstrictive substances (e.g., caffeine) can facilitate awakening [2].

Prolonged sleep deprivation induces a substantial decrease in core body temperature and, as shown in animal experiments, can lead to thermoregulatory failures [3]. It is an open research task to monitor the response of the circadian curve to prolonged sleep restriction and to verify the hypothesis that sleep deprivation flattens circadian rhythms. We aim at monitoring patients for periods ranging from 6 days up to two weeks with prescribed sleep schedule (including prolonged sleep restriction) and check the impact on their circadian rhythms. This goal imposes a first important system requirement: the system should support uninterrupted operation for at least two weeks.

B. Relating Skin Temperature Variations to Cognitive, Emotional, and Psychological States

Emotions induce sympathetic activation that induces cutaneous vasoconstriction [4]. Psychologists normally use skin conductance as a measure to assess the cutaneous sympathetic activation: vasoconstriction induces sweating, and hence the resistance of the skin decreases. Skin conductance is typically sampled at 400 Hz using a time window of 1.5 to 6.5 seconds after the stimulus. We want to verify if also distal skin temperature changes at timescales of seconds due to changing emotional states.

Dittmar et al. [5] presented preliminary results showing that the skin temperature measured at the temple decreases instantaneously as soon as the brain starts to solve an arithmetic task. We want to confirm those results and verify if brain activity produces a decrease of skin temperature by monitoring the temple skin temperature of patients.

III. Related Work

In the last decade, an increasing number of wearable biomedical sensors have been used for diagnosis and treatment of diseases, and body sensor networks have been successfully applied to several health-care applications. Lorincz, Patel, et al. [6], [7] have proposed Mercury, a wearable sensor-network platform for high-fidelity motion analysis

that has been used to monitor motor fluctuations in patients with neuromotor disorders, epilepsy, and Parkinson's disease. Malan et al. [8] developed CodeBlue: a sensor-network infrastructure for emergency medical care, which tracks patients throughout the medical response process, from the accident location over ambulances to hospitals. Differently from these efforts that focus on health-care and emergency-care applications, our work uses body sensor networks to support medical research by allowing long-term and accurate measurements in realistic settings.

Several studies have analyzed the circadian rhythms using various measurement approaches. Methods such as the measurement of salivary melatonin, cortisol levels, urinary 6-sulfatoximelatonin, midstream urine temperatures, vaginal [9] and core body temperature by means of rectal probes, and blood pressure have been used as indicators of biological internal timing. However, most of these methods require specialized laboratories, or they cause frequent disturbances that are unacceptable to most patients [10], [11]. Similarly to the above studies, we also aim to study circadian rhythms, but in more realistic home environments and for long-time periods in a seamless way.

Recent studies have shown how the circadian rhythms can also be monitored under constant routine conditions and free living conditions [10], [12], [13]. This offers the opportunity to use continuous skin temperature monitoring of subjects in their natural environment to assess circadian rhythmicity of thermoregulation and hence sympathetic activity for several days. Also the use of actimetry as a method to evaluate circadian rhythmicity in supportive home environments has been proposed, but the obtained measurements are strongly affected by external factors (e.g., the removal of the sensor for taking a shower before going to bed or a car ride might be wrongly identified as a sleeping period). Similarly to the above studies, we also aim to study circadian rhythms in supportive home environments. In particular, we apply wireless measurements of skin temperature to monitor the circadian activity.

The measurement of skin temperature by means of wireless devices or wireless data loggers has recently gained popularity among medical researchers. Chen et al. [14] have built a prototype belt for non-invasive neonatal temperature monitoring: the system they developed uses NTC temperature sensors and achieves an accuracy of about 0.1^oC. Van Marken et al. [15] recorded the human skin temperature on hands and feet using iButtons [16], and Sarabia et al. [10] used the same tool to investigate circadian rhythmicity through the measurement of wrist temperature. The DS1921H/Z iButton [16] is a miniaturized digital thermometer that measures temperature with a resolution of $1/8^oC$ with an accuracy of $\pm 1^oC$. According to the specifications [16], up to 2048 temperature values sampled at equidistant intervals ranging from 1 to 255 minutes can be stored. While the iButtons are small, their lifetime is too short to provide the long-term measurements that we need for our application. Also, the iButton is a data logger, and therefore does not offer real-time feedback to the medical unit. Furthermore, in order to be able to relate variations of skin temperature to cognitive, emotional, and psychological states, a much higher sampling rate is needed. The system we design provides higher accuracy and longer lifetime with respect to the iButtons, and can also communicate with other nodes and form a body sensor network, hence providing real-time feedback to the caregivers.

Modifying the sampling rate, we also use our system for relating variations of skin temperature to cognitive, emotional, and psychological states. Similar work has been done by Brown et al. [17], who have built a modular low-power body area network for monitoring autonomic nervous system responses during stress and emotion periods. They successfully used heart rate and skin conductance measurements to correctly classify the emotional state of patients, reaching a classification accuracy up to 64%. Differently from them, we want to analyze the impact of emotions on peripheral skin temperature.

There are a number of further research activities that could benefit from our non-invasive accurate temperature measurement tool, such as investigations of the relationship of skin temperature changes to the emotions accompanying music [18] or videos [19], as well as studies of the influence of solar radiation on skin temperature [20].

IV. Requirements, Architecture, and Prototype

From the applications outlined in Sect. II we first derive a set of key requirements. We then describe the architecture of our body sensor network that is driven by the requirements. Finally, we briefly describe the sensor node platform we used and the prototype we built.

A. Requirements and Challenges

We derive requirements from the applications described earlier in the paper, and point out how these requirements affect the design of the system.

Non-invasiveness. The sensors have to be worn continuously at different places on the body over weeks. Therefore, the sensor nodes have to be small and lightweight and must not constrain the test subjects in their daily activities. In order to achieve a small node size, the energy budget (battery) and computational resources of sensor nodes are severely constrained. In order to allow test subjects free movement, a wireless solution is needed.

Long Lifetime. Monitoring the circadian rhythms requires the system to be run uninterruptedly over several weeks. Specifically, we require a lifetime of at least three weeks when taking one sample every 30 seconds. Due to the limited battery capacity, all system components must be optimized for energy efficiency by putting hardware into power-saving sleep modes as often as possible.

High Accuracy and Flexible Sampling Rates. For monitoring circadian rhythms, temperature measurements need to have an accuracy of at least 0.05°C over a typical skin temperature range of 16-42°C. As different applications require different sampling rates in the range from 0.01 Hz (circadian rhythms) to 10 Hz (emotions), the sampling frequency should be configurable.

Robustness. The system should be operational over weeks without interruption and without requiring manual intervention. This is challenging, as the sensor nodes worn on the body (e.g., on the back of the hands) may be exposed to extreme environmental conditions such as water (rain, washing hands, shower), mechanical shock, environmental temperature variations, but also interference from wireless transmitters operating in the same frequency band. The sensor nodes therefore have to be packaged and fixed to the body in a robust manner and use communication protocols that adapt to wireless interference.

Real-time Feedback. Running a medical study with test subjects over weeks is costly and requires substantial preparation. Therefore, the data is very precious. As the subjects wear the sensors over weeks, it is required that the researchers have online and real-time access to the collected data, for example to detect and fix problems early (fixing loose sensors), or to detect cheating events (even though test subjects are paid, they often do not comply with unpleasant instructions such as sleeping only four hours per day).

Network size. For investigating circadian rhythms, we need to measure distal skin temperature at the back of the hands, at the back of the feet, at the trunk of the body (e.g., above the liver), and the core body temperature (e.g., in the ear). Therefore, we need a wireless body area network of up to ten sensor nodes.

Self-Test. To maximize the quality of the collected data, we want the body sensor network to detect certain failure events (such as a loose sensor) by analyzing the sensor output and to give automatic feedback to the test subject to fix the problem.

Diary. Medical researchers are interested in correlating the temperature measurements with the activities of the test subjects such as going to bed, getting up, sitting, walking, etc. Hence, the BSN should also detect and record certain activities (e.g., light sensor to detect darkness, accelerometer to detect posture and movements). For activities that are hard to recognize automatically, a simple user interface (e.g., button) should be provided to allow the user to indicate the begin of a certain activity (e.g., food intake). This requires multiple heterogeneous sensors to be connected to a mote.

Compensation for Ambient Conditions. Traditionally, skin temperature measurement studies are performed in an idealized lab setting with constant environmental conditions, in particular with a constant room temperature. However, we are aiming at long-term studies in real-world settings, where environmental conditions are changing. In particular, the environmental temperature fluctuations have a profound impact on the thermoregulation of the body. Also, environmental temperature may differ across the body (one foot sticking out the blanket in bed). Hence, we also need to measure the environmental temperature distribution across the body and compensate the skin temperature measurements by means of appropriate models. Measuring environmental temperature itself is not easy, as sensors worn on the body are influenced both by the skin temperature and the environmental temperature. Hence, we need at least two temperature measurements (on skin, above skin) at every measurement point on the body to solve an equation system of two unknowns: skin temperature and environmental temperature.

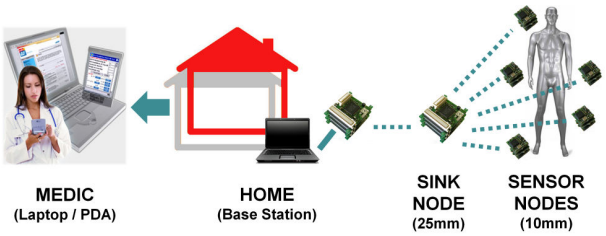

Figure 1. Architecture of our BSN and back-end infrastructure.

In the remainder of this paper we describe the design and implementation of a BSN meeting these requirements. Our focus will be on the basic ones – especially on how to realize very accurate temperature measurements. Advanced features such as self-testing, diary, and compensation for ambient conditions are part of ongoing and future work.

B. Architecture

The architecture of our body sensor network is illustrated in Figure 1. The subject wears multiple, small wireless *sensor nodes* on the body. Several sensors (including two thermistors to measure the temperature on and above the skin) are attached to each sensor node. Due to the small size, these sensor nodes are relatively limited in their energy supply, storage, and computational resources. Therefore, we include a more powerful *sink node* in our network that is larger and therefore offers more resources and power. This sink node can be worn in the pocket, for example. The sink node includes additional sensors (e.g., an accelerometer for activity recognition) and user interfaces (e.g., button and LEDs). The sink node and the sensor nodes form a wireless network with a star topology, where the sensor nodes collect a number of samples and send it to the sink node. The sink node has a large memory and logs the received samples. This heterogeneous architecture [21] offers both unobtrusive measurements by means of small sensor with limited functionality, and extensive storage and computational power by means of more powerful sink node that can fit in a pocket without impacting user comfort.

Whenever the subject enters the range of a *base station* installed at home, the sink node forwards collected samples to the base station wirelessly. The latter consists of a laptop

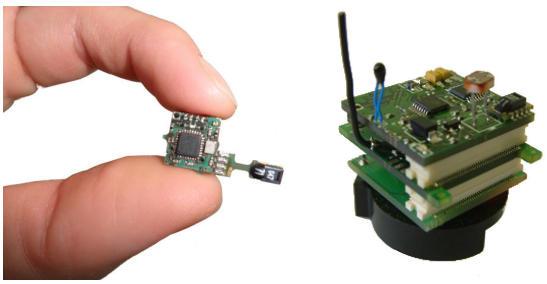

(a) Tyndall 10mm node (b) Tyndall 25mm node

Figure 2. Wireless sensor nodes used in our body sensor network.

wired to another sensor node to allow wireless communication between the sink node and the laptop. The laptop is also connected to the Internet, allowing remote access to the collected data for the medic. Typically, the user returns home at least once per day, such that the medic has access to the data with a latency of at most one day. When the patient is at home, the medic has instant access to the data.

In some applications with low sampling rates, the sensor nodes may store enough samples in their small memories, so that a sink node is not needed. Instead, the sensor nodes transmit collected data to the base station directly whenever the subject wearing the body sensor network is in range on the base station.

C. Hardware Platforms

We use the Tyndall 10mm [22] and 25mm [23] to implement our architecture. Our choice was motivated by the fact that the 10mm node matches the size requirements for the sensor nodes, while the 25mm node is powerful enough to act as a sink node. Both nodes can communicate with each other as they use compatible radios. Furthermore, the Tyndall platforms are modular: both nodes are composed of one or more stackable PCB layers. The main layer contains the microcontroller and the radio transceiver. Additional stackable layers contain sensor interfaces, storage, and additional radio modules. Compared to the typical monolithic node designs, this modular approach allows us to customize the hardware according to our specific application requirements.

The 10mm node [22] (Figure 2(a)) is the smallest node of the Tyndall family: each layer is roughly 10x10x3 mm big. The node has been designed to support very low-power operation for applications with low duty cycles, with a sleep current of only 3.3μA [22]. Its small size, energy-efficiency, and low cost make the node suitable for building body sensor networks. The basic layer includes a Nordic nRF9e5 RF transceiver operating in the 433 MHz frequency band, as well as an 8051-compatible embedded microcontroller. The output power of the radio transceiver is adjustable up to 10 dBm and the typical sensitivity threshold is -100 dBm. The nRF9e5 microcontroller supports voltage supply down to 1.9V and provides a 10-Bit (extensible to 12) ADC converter that supports 100k samples per second. The microcontroller includes a 256-byte data RAM, and the bootstrap loader is

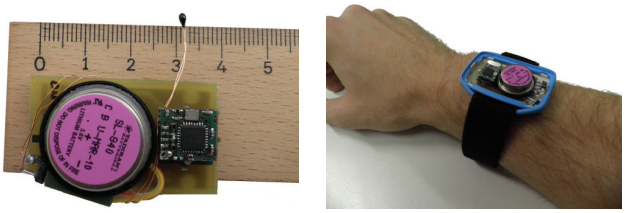

(a) Prototype Board (b) Packaging (top removed)

Figure 3. Our body sensor node prototype and its packaging.

contained in a 512-byte ROM. The user program is loaded into the first half (4 kB) of an Atmel AT25640A EEPROM, and the second half (4 kB) can be used for data storage.

The Tyndall 25mm [23] (Figure 2(b)) is a more powerful node, and has been used in the last years for marine applications, environmental monitoring of plants and smart spaces, human interfacing, movement tracking, health-care, and well-being applications [24]. The basic layer incorporates an Atmel ATmega128 microcontroller and a Nordic nRF905 radio transceiver operating in the 433 MHz frequency band that is compatible with the radio used by the 10mm node. The ATmega128 is an 8-bit microcontroller with 128 Kbytes of in-system programmable Flash program memory, 4 kB EEPROM, 4 kB internal SRAM, and a 10-bit ADC.

D. Prototype

Based on the Tyndall 10mm nodes, we developed a prototype of the body sensor node as shown in Fig. 3(a). The hardware consists of a 10mm main layer, MF51E [25] Negative Temperature Coefficient (NTC) thermistors, conditioning circuitry on a custom PCB to connect the sensors to the microcontroller (described in the next section), and a battery. Despite using a Lithium Thionyl primary battery (Tardiran SL-840 with a capacity of 420 mAh) that offers a very high energy density, the battery dominates the size of the hardware. The electronics are packaged in an OKW Minitec Enclosure (Fig. 3(b)) that can be fixed to arms or legs with a strap.

The software developed for the sensor node samples temperature at a configurable rate and groups readings in packets of 30 bytes that are sent wirelessly to the sink node. We use acknowledgements to monitor connectivity with the sink node. If the sensor node does not receive an acknowledgment, it stores the packet (and all future data) in local EEPROM and periodically reattempts to send the data to the sink. In order to minimize the amount of retransmissions and hence save energy, we use a linear truncated backoff, which increases the waiting time linearly with the amount of consecutive failures. As soon as the communication with the sink node succeeds again, the sensor node tries to quickly drain its EEPROM to the sink. In case the EEPROM is filled before the communication with the sink is restored, new sensor readings are discarded. We timestamp each reading so that the sink node can reconstruct the time sequence.

V. Accurate Temperature Measurements

Obtaining temperature measurements with an accuracy in the order of a few hundredths degrees Celsius turned out to be challenging. In order to exploit the full resolution of the analog-to-digital converter (ADC), an active conditioning circuitry is needed. The latter has to be parameterized such that the relevant temperature range of 16-42°C maps to the full input voltage range of the converter. Further, we need to calibrate the whole measurement circuit in order to reduce systematic measurement errors.

A. Thermistors

A thermistor is a temperature-dependent resistor with a non-linear mapping of resistance R to temperature T (in Kelvin) that can be described by the Steinhart-Hart equation with device-dependent coefficients a, b, and c:

$$\frac{1}{T} = a + b\ln(R_{Th}) + c\ln^3(R_{Th}), \tag{1}$$

We use as a sensor a thermistor with a Negative Temperature Coefficient (NTC) that can also be modeled by the simpler B-parameter equation:

$$T = \frac{B}{\ln(R_{Th}/r_\infty)} \tag{2}$$

where:

$$r_\infty = R_0 e^{-B/T_0} \tag{3}$$

B is the so-called B-parameter, and R_0 is the resistance at temperature T_0. Eq. 2 is a special case of Eq. 1 where $a = \frac{1}{T_0} - \frac{1}{B}\ln(R_0)$, $b = \frac{1}{B}$, and $c = 0$. By setting $c = 0$ in the Steinhart equation, the $\ln^3(R_{Th})$ term is omitted. The error introduced by this omission is negligible, as for typical R_{Th}-values, $c \approx 10^{-8}$.

B. Conditioning Circuit

In order to maximize the ADC resolution, we need a conditioning circuit that maps the thermistor resistance range $[R_{min}, R_{max}]$ to a voltage range $[0, V_{max}]$ that fully exploits the input range of the ADC (with V_{max} being the maximum ADC input voltage). With a simple passive voltage divider, an input voltage of zero cannot be obtained, as the thermistor resistance is always non-zero. Therefore, we adopt the solution shown in Fig. 4 based on an operational amplifier, whose output voltage range can be adjusted to match the required range through the selection of appropriate resistors values.

The microcontroller on the Tyndall 10mm platform offers an external voltage reference for ADC conversion, *Aref*, limited to a maximum value of 1.5V that can be obtained by scaling the supply voltage by means of a voltage divider. The voltage applied on *Aref*, V_{Aref}, determines the maximum ADC input value, i.e., $V_{max} \leq V_{Aref}$. Through this configuration we obtain temperature measurements independent of the supply voltage, as we later discuss in this section.

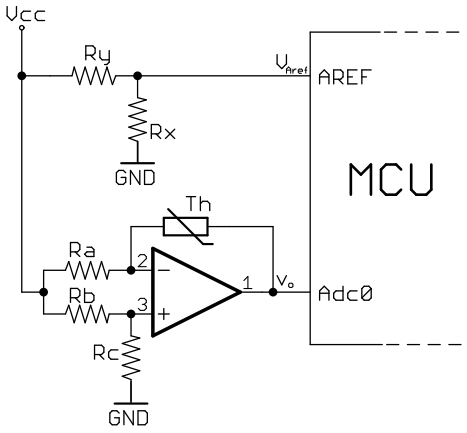

Figure 4. The complete circuit diagram.

The operational amplifier changes its output voltage v_o in order to compensate the voltage difference present on its inputs V_+ and V_-. Consequently, considering that the current flowing into the op-amp can be neglected due to its high input impedance, the two branches $R_a - R_{Th}$ and $R_b - R_c$ can be considered as a voltage divider. With $V_- = V_+$, we obtain the following linear relationship between the resistance R_{Th} of the thermistor and output voltage v_o:

$$v_o(R_{Th}) = V_{cc}\Big(\frac{R_a R_c}{R_a(R_b + R_c)} - R_{Th}\frac{R_b}{R_a(R_b + R_c)}\Big) \tag{4}$$

To select the proper values for R_a, R_b, R_c, we need to solve the equation (4) for the values of the resistors under the following two boundary conditions:

$$\begin{cases} v_o(R_{max}) = 0 \\ v_o(R_{min}) = V_{max} \end{cases} \tag{5}$$

The equation system of (4) and (5) is underconstrained as we have three unknowns R_a, R_b, R_c but only two equations. However, since R_b and R_c form a voltage divider whose output V_+ depends only on the ratio $\frac{R_c}{R_b+R_c}$, we effectively have only two unknowns. We therefore solve the equation system assuming $R_b = R_a$, but we consider them separately in the remainder of the paper since their actual values may differ slightly due to the production tolerance.

One important aspect that affects accuracy is the self-heating of the thermistor (known as the *Joule effect*) due to the current flowing through it. The heat dissipated by the thermistor is a function of the current flowing through it and its resistance. The resistance in turn is affected by the measured temperature. We devise a calibration procedure in the following section to compensate variations in self-heating due to changes of environmental temperature. The current flowing through the thermistor depends on V_{cc} (but not on the resistance of the thermistor). Therefore we use a Torex XC6215 voltage regulator to produce a constant V_{cc} of 3.3V. According to the datasheet [26], the regulator has a swing on the output voltage smaller than ± 0.01V. Therefore,

the inaccuracy of temperature measurement due to the self-heating effect caused by changes in battery voltage is in the order of ± 0.00014°C, two orders of magnitude less than our target accuracy.

Combining the conditioning circuit with a voltage divider to provide the ADC voltage reference V_{Aref} as shown in Fig. 4, we obtain a linear relationship between the thermistor resistance R_{Th} and the digital ADC output value D_{adc} as follows. D_{adc} is proportional to v_o according to $\frac{D_{adc}}{2^N} = \frac{v_o}{V_{Aref}}$, where N is the number of bits of D_{adc}. By solving (4) for R_{Th} with $V_{Aref} = V_{cc} \cdot \frac{R_x}{R_x + R_y}$, we obtain:

$$R_{Th} = \frac{R_a R_c}{R_b} - \frac{R_x}{R_x + R_y} \cdot \frac{R_a(R_b + R_c)}{R_b} \cdot \frac{D_{adc}}{2^N} \quad (6)$$

Note that R_{Th} is independent from the supply voltage.

C. Calibration

To simplify the following discussion, we rewrite (6) as:

$$R_{Th} = q - \varphi \cdot m \quad (7)$$

where $q = \frac{R_a R_c}{R_b}$, $m = \frac{R_x}{R_x + R_y} \cdot \frac{R_a(R_b + R_c)}{R_b}$, and $\varphi = \frac{D_{adc}}{2^N}$.

Equations (2) and (7) describe the complete mapping from ADC output φ to measured temperature T. This mapping obviously depends on the values of the resistors R_* as well as on the thermistor coefficients B and r_∞. Although the latter two values can be obtained from the data sheet of the thermistor and the resistor values are known, the resulting measurement accuracy is not sufficient due to the tolerance of $\pm 0.5\%$ of the thermistor parameters and $\pm 1\%$ of the chosen resistors.

We therefore need a simple, yet accurate, calibration procedure of the thermistor and the conditioning circuit. We came up with a solution that just requires a glass of water and a precision thermometer [27].

We place the thermometer and the thermistor within 1 cm distance inside a glass (diameter 85mm, height 220mm) filled with one liter of water. The water has an initial temperature of about 42°C and cools down naturally until 16°C. This operation requires more than 2 hours, in which, on average, the temperature of the water drops of 0.01°C every 2.8 seconds. As the response time of our calibration thermometer is one second, we have enough time to characterize the thermistor with the desired accuracy.

While the water slowly cools down, the thermometer and the ADC output φ are sampled simultaneously at regular intervals to obtain data points (φ_i, T_i). Plugging such a data point into equations (2) and (7), we obtain one equation with our calibration parameters as unknowns. Doing this for many data points, we obtain an overconstrained equation system than can be solved for the calibration parameters by means of least squares optimization. Specifically, we can combine (2) and (7) and rewrite as follows:

$$Q - \varphi \cdot M = e^{B/T} \quad (8)$$

where $Q = \frac{q}{r_\infty}$ and $M = \frac{m}{r_\infty}$. Using the B parameter from the data sheet of the thermistor, we have to solve for just two calibration parameters Q and M. As r_∞ depends on B (see Eq. 3) and as Q and M depend on r_∞, we also compensate the inaccurate value for B obtained from the data sheet.

Inserting n data points (φ_i, T_i) into (8), we obtain the following overconstrained linear equation system with two variables M and Q, and n equations:

$$\begin{bmatrix} -\varphi_1, & 1 \\ \vdots & \vdots \\ -\varphi_n & 1 \end{bmatrix} \cdot \begin{bmatrix} M \\ Q \end{bmatrix} = \begin{bmatrix} e^{B/T_1} \\ \vdots \\ e^{B/T_n} \end{bmatrix} \quad (9)$$

Rewriting this as $A \cdot x = Y$, we obtain a solution $x = [M, Q]$ that minimizes $(A \cdot x - Y)^2$ by means of least squares optimization. This optimal solution can be found by solving the linear system of two equations $(A^\top A)x = A^\top Y$. Plugging the obtained calibration parameters Q, M, and B into (8), we can now compute an accurate estimate of temperature T given an ADC sample φ.

An evaluation showed that the resulting accuracy varies over the temperature range [16,42]°C. We conjecture that this is due to the self-heating effect which is not explicitly modeled in our equations. We therefore split the temperature range into two sub-ranges [16,32.5]°C and [32.5,42]°C and obtain separate calibration parameters (M_r, Q_r) for each range r. This results in an accuracy in the order of $0.02°C$ over the whole range, as described in Section VI-A.

D. Adaptive Sampling

The calibration process eliminates systematic measurement errors to a large degree. However, we still have to deal with noise. Assuming that noise can be modeled by a Gaussian distribution, we can take multiple samples and compute the average in order to reduce the noise. However, taking multiple samples also increases the consumption of precious energy. We therefore want to select the minimum number of samples that allows us to meet the accuracy requirement of the application.

To facilitate this adaptive sampling, we employ an empirical approach to obtain a mapping between number of samples and resulting accuracy. Using the same setup as for calibration, i.e., glass of warm water with thermometer and thermistor placed next to each other, we obtain a new series of data points (φ_i, T_i). As the water is cooling down very slowly, we obtain multiple data points $i_1, i_2, ...$ with the same value for T, i.e., $T_{i_1} = T_{i_2} = ...$, but with different values for φ, i.e., $\varphi_{i_1} \neq \varphi_{i_2} \neq ...$ due to measurement noise. For a given number of samples N we now compute an averaged data point $(T_i, \frac{1}{N} \sum_{k=1...N} \varphi_{i_k})$.

Using the previously computed calibration parameters Q, M, B, and the averaged data point, we now compute the measured temperature T using (8). By repeating the experiment, we obtain multiple measured temperatures for a given

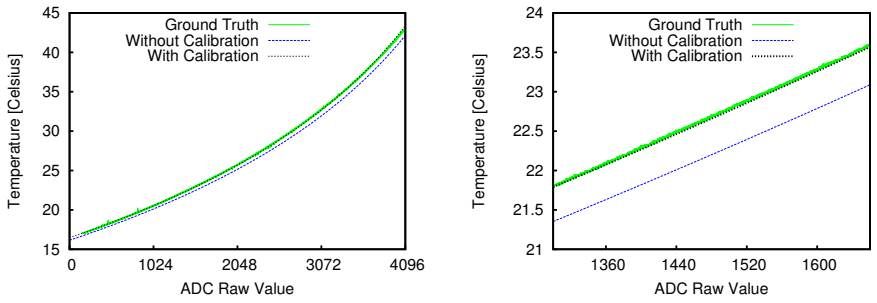

(a) Full Range (b) Zoom-in

Figure 5. Performing calibration improves the accuracy obtained when using the nominal values of the thermistor.

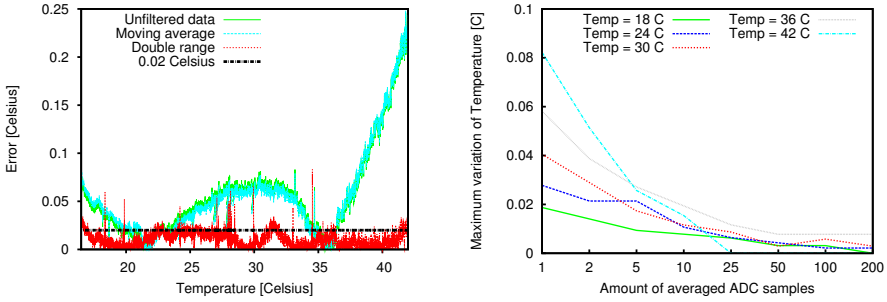

(a) Accuracy (b) Noise

Figure 6. Accuracy and noise as a function of the number of averaged samples.

ground truth temperature. By subtracting the minimum from maximum measured temperature, we obtain a measure for magnitude of the noise for a given ground truth temperature and a given number of samples N. The resulting graph in Fig. 6(b) (see evaluation for details) can then be used to select the number of samples in order to obtain a given accuracy.

VI. Evaluation

In this section, we evaluate the accuracy of temperature measurements with our prototype and run preliminary experiments with a test subject wearing the body sensors. We can identify the circadian rhythms from skin temperature measured at the non-dominant hand over 24 hours. We also show the high impact of environmental temperature on the skin temperature readings. We further carry out an experiment to show the impact of mental activity on the skin temperature measured at the temple.

A. Accuracy

As detailed in Section V-C, we calibrate our system by letting a glass of water cool down from 42°C to 16°C while continuously sampling the ADC, computing the average of 50 consecutive ADC samples over a duration of 12.5 ms (i.e., effective sampling rate of 80 Hz), and send the result to the sink node. A laptop logs the readings from the thermometer and from the sink node via serial interfaces. We obtain calibration parameters M = 140.31 and Q = 837530.87. Figure 5 compares the temperature readings obtained with the thermometer and the thermistor, and also shows the obtained temperature when using calibration parameters from the data sheet. Figure 5(b) shows how calibration improves the accuracy by up to approximately 0.5°C and is therefore indispensable for obtaining an accuracy below 0.1°C.

Using the same setup, we measure the accuracy over the temperature range of interest 16-42°C using three different calibration approaches, and the model described in Section V-C. Figure 6(a) shows the results. When using an unfiltered dataset, i.e., the original set of collected data points (φ_i, T_i), the error varies in the range [0,0.25]°C. The same applies for a filtered dataset, in which we perform a moving average over 250 samples over the original data points. For this reason, we split the dataset into two sub-ranges and compute different calibration parameters M and Q for the different subsets as described in Sect. V-C. We choose as cut-off point between the two sub-ranges 32.50°C, which maximizes the accuracy. By using the resulting calibration parameters for the sub-ranges, the error is less than 0.02°C over the temperature range of interest.

Finally, we assess the variability of the measurements due to noise as a function of the number of samples used for averaging as described in Sect. V-D. The results in Fig. 6(b) show that $N = 50$ samples represents a good tradeoff between accuracy and energy efficiency. The figure can also be used to find the number N of samples required to limit the noise to a certain amount required by the application.

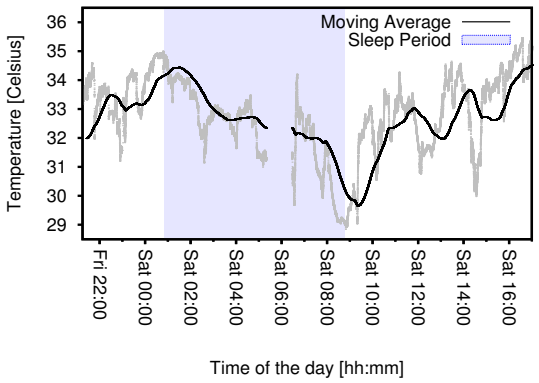

Figure 7. Monitoring of the circadian rhythms through a continuous measurement of the hand temperature.

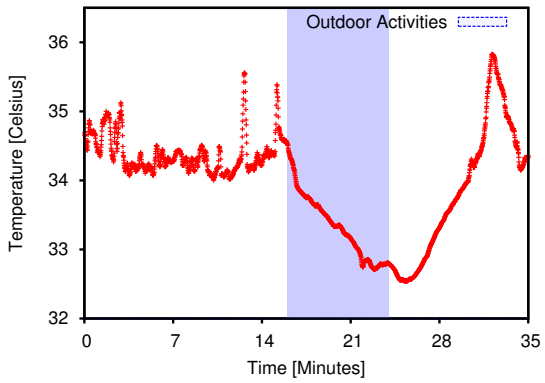

Figure 8. Impact of environmental temperature variations on skin temperature. When switching from indoor to outdoor environments and vice versa, we see a variation in skin temperature up to several degrees Celsius.

B. Monitoring Circadian Rhythms

We instruct a 24-years old male subject in normal health conditions to wear our body sensor network and monitor the skin temperature of his non-dominant hand over a period of 24 hours. The subject is living his normal life. Our goal is to verify whether we can identify circadian rhythms from continuous hand temperature measurements outside of the controlled temperature environment of a lab.

Figure 7 shows the raw data collected between a Friday evening and a Saturday evening at a sampling rate of 1Hz. The small interruption of connectivity at 6 AM is due to a communication failure. As we sample the temperature every second, we can notice variations due to user mobility, emotional status, and due to changes in environmental temperature. If we filter the data using a moving average over 5000 samples, we can see the expected trend over the course of a day. In the evening, as a result of vasodilatation, we see an increase of temperature, followed by a decrease as soon as the patient goes to bed. In the following morning, the temperature starts rising again. This proves that our sensor node does a commendable job in detecting the circadian rhythm through hand temperature measurements.

As mentioned in Section IV-A, the environmental temperature has a strong impact on skin temperature. In particular, patient mobility causes frequent changes of the ambient context including environmental temperature. This is even more visible when the patient moves from indoor to outdoor environments and vice versa. Figure 8 shows how the skin temperature is affected by a variation up to more than $2°C$ when the patient spends a few minutes outdoor (data is collected during autumn in north Germany). For this reason, it is important to compensate the impact of ambient temperature as discussed in Sect. IV-A. We will address this difficult issue in future work.

C. Monitoring Mental Activity

We also measure the skin temperature at the temple of a 24-year old male subject in normal health conditions and investigate the impact of mental activity on its temple skin temperature. We let the patient wear the sensor node and relax on an armchair. After fixed periods of time, we let the patient relax or ask him to interact, read, write, and perform mental tasks. We sample the temperature at 80 Hz; Figure VI-C shows the collected data. Contrary to the results of Dittmar et al. [5], we can neither see sudden variations of temperature, nor can we unequivocally say that the brain activity decreases the skin temperature measured at the temple at timescales of hundreds of milliseconds.

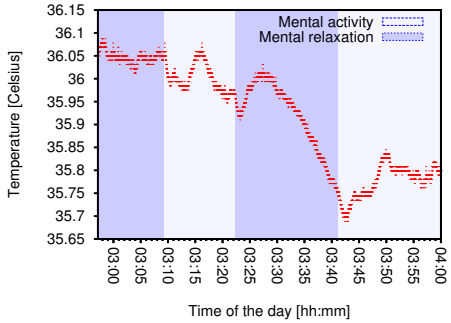

Figure 9. Impact of mental activity on temple skin temperature.

VII. Conclusions and Future Work

Body sensor networks have the potential to revolutionize medical research. Non-invasive and accurate measurements of body temperature in a continuous fashion over weeks in realistic environments can substantially improve the quality of data available to medical researchers such as psychophysiologists and chronobiologists.

In this paper, we design a body sensor network architecture and nodes that can accurately measure the body temperature in a non-invasive fashion and send real-time feedback to the medic. Our design guarantees a long battery lifetime, hence uninterrupted operations for several weeks.

We use this body sensor network to run a preliminary study of the circadian rhythms over a 24-hour period, and show that starting from measurements of hand temperature

in non-constrained environments we can see the expected temperature fluctuations. We further analyze the impact of ambient temperature variations on skin temperature and verify whether mental activities affect the skin temperature measured at the temple.

Providing accurate temperature measurements over long periods of time with a small node as described in this paper is the cornerstone of our work. Next we will focus on advanced self-organization functionalities such as self-testing, adaptive communication protocols, automatic compensation for environmental conditions, or automatic generation of a diary of activities.

ACKNOWLEDGMENTS

This research has been supported by the DFG-funded (German Research Foundation) Cluster of Excellence 306/1 "Inflammation at Interfaces". This work has been partially financed also by CONET, the Cooperating Objects Network of Excellence, funded by the European Commission under FP7 with contract no. FP7-2007-2-224053.

REFERENCES

[1] A. A. Romanovsky, "Thermoregulation: some concepts have changed. Functional architecture of the thermoregulatory system," *Am J Physiol Regul Integr Comp Physiol 292*, vol. R37-R46, Sep. 2006.

[2] K. Kräuchi, C. Cajochen, E. Werth, and A. Wirz-Justice, "Warm feet promote the rapid onset of sleep," *Nature*, vol. 401, pp. 36–37, 1999.

[3] J. Vaara, H. Kyrolainen, M. Koivu, M. Tulppo, and T. Finni, "The effect of 60-h sleep deprivation on cardiovascular regulation and body temperature," *Eur. J Appl. Physiol*, vol. 105, pp. 439–444, 2009.

[4] W. Blessing, "Lower brainstem pathways regulating sympathetically mediated changes in cutaneous blood flow," *Cell Mol Neurobiol.*, vol. 23, no. 4-5, pp. 527–538, Oct. 2003.

[5] A. Dittmar, C. Gehin, G. Delhomme, D. Boivin, G. Dumont, and C. Mott, "A Non Invasive Wearable Sensor for the Measurement of Brain Temperature," in *Proc. of the 28th IEEE EMBS Intern. Conf.*, New York City, USA, Aug. 2006.

[6] S. Patel, K. Lorincz, R. Hughes, N. Huggins, J. Growden, D. Standaert, M. Akay, J. Dy, M. Welsh, and P. Bonato, "Monitoring Motor Fluctuations in Patients With Parkinson's Disease Using Wearable Sensors," *IEEE Trans. on Information Technology in Biomedicine*, vol. 13, no. 6, Nov. 2009.

[7] K. Lorincz, B. rong Chen, G. W. Challen, A. R. Chowdhury, S. Patel, P. Bonato, and M. Welsh, "Mercury: A Wearable Sensor Network Platform for High-fidelity Motion Analysis," in *Proc. of the 7th Conference on Embedded Networked Sensor Systems (SenSys)*, Berkeley, CA, USA, Nov. 2009.

[8] D. Malan, T. Fulford-Jones, M. Welsh, and S. Moulton, "CodeBlue: An ad-hoc sensor network infrastructure for emergency medical care," in *Proc. of the Workshop on Appl. of Mobile Emb. Systems (WAMES)*, Boston, USA, Jun. 2004.

[9] J. J. Rodrigues, J. Caldeira, and B. Vaidya, "A Novel Intrabody Sensor for Vaginal Temperature Monitoring," *Sensors*, vol. 2009, no. 9, pp. 2797–2808, Apr. 2009.

[10] J. Sarabia, M. Rol, P. Mendiola, and J. Madrid, "Circadian Rhythm of Wrist Temperature in Normal-living Subjects: a Candidate of New Index of the Circadian System," *Physiology and Behavior*, vol. 2008, no. 95, pp. 570–580, Aug. 2008.

[11] S. Ancoli-Israel, R. Cole, C. Alessi, M. Chambers, W. Moorcroft, and C. Pollak, "The role of actigraphy in the study of sleep and circadian rhythms," *Sleep*, vol. 26, no. 3, pp. 342–392, 2003.

[12] K. Kräuchi and A. Wirz-Justice, "Circadian rhythm of heat production, heart rate and skin and core temperature under unmasking conditions in men." *Am. J Physiol*, vol. 267, pp. R819–R829, 1994.

[13] M. Varela, D. Cuesta, J. A. Madrid, J. Churruca, P. Miro, R. Ruiz, and C. Martinez, "Holter Monitoring of Central and Peripheral Temperature: Possible Uses and Feasibility Study in Outpatient Settings," *Journal of Clinical Monitoring and Computing*, vol. 2009, no. 23, pp. 209–216, May 2009.

[14] W. Chen, S. Dols, S. B. Oetomo, and L. Feijs, "Monitoring Body Temperature of Newborn Infants at Neonatal Intensive Care Units Using Wearable Sensors," in *Proceedings of the 5th International Conference on Body Area Networks (BodyNets)*, Corfu Island, Greece, Sep. 2010.

[15] W. V. M. Lichtenbelt, H. Daanen, L. Wouters, R. Fronczek, R. Raymann, N. Severens, and E. V. Someren, "Evaluation of Wireless Determination of Skin Temperature using iButtons," *Physiology and Behavior*, no. 88, pp. 489–497, Apr. 2006.

[16] Maxim Integrated Products, Inc., "DS1921H/Z: High-Resolution Thermochron iButton," Aug. 2009.

[17] L. Brown, B. Grundlehner, J. van de Molengraft, J. Penders, and B. Gyselinckx, "Body Area Network for Monitoring Autonomic Nervous System Responses," in *Proce. of the 3rd Intern. Conf. on Pervasive Computing Technologies for Healthcare (PervasiveHealth)*, London, UK, Apr. 2009.

[18] R. A. McFarland, "Relationship of Skin Temperature Changes to the Emotions Accompanying Music," *Biofeedback and Self-Regulation*, vol. 10, no. 3, 1985.

[19] S. E. Rimm-Kaufman and J. Kagan, "The Psychological Significance of Changes Skin Temperature," *Motivation and Emotion*, vol. 20, no. 1, 1996.

[20] K. Blazejczyk, "Influence of Solar Radiation on Skin Temperature in Standing and Walking Subjects Outdoors," in *Proceedings of the 8th International Conference on Environmental Ergonomics*, San Diego, CA, USA, Oct. 1998, pp. 57–60.

[21] S. Harte, E. M. Popovici, B. O'Flynn, and C. O'Mathuna, "THAWS: Automated Design and Deployment of Heterogeneous Wireless Sensor Networks," *WSEAS Transactions on Circuits and Systems*, vol. 7, no. 9, Sep. 2008.

[22] S. Harte, B. O'Flynn, R. Martínez-Catalá, and E. Popovici, "Design and Implementation of a Miniaturised, Low-Power Wireless Sensor Node," in *Proceedings of the 18th European Conference on Circuit Theory and Design (ECCTD)*, Seville, Spain, Aug. 2007, pp. 894–897.

[23] J. Barton, G. Hynes, B. O'Flynn, K. Aherne, A. Norman, and A. Morrissey, "25mm Sensor-actuator Layer: a Miniature, Highly Adaptable Interface Layer," *Sensors and Actuators A: Physical*, vol. 132, no. 1, pp. 362 – 369, 2006.

[24] B. O'Flynn, A. Lynch, K. Aherne, P. Angove, J. Barton, S. Harte, and C. O'Mathuna, "The Tyndall Mote: Enabling Wireless Research and Practical Sensor Application Development," in *Adjunt Proceedings of Pervasive*, Dublin, Ireland, May 2006.

[25] Cantherm Ltd., "MF51E: High Precision NTC Thermistors for Extremely Accurate Temp. Measurement," Mar. 2006.

[26] Torex Semiconductor Ltd., "XC6215 Series: Low Power Consumption Voltage Regulator with ON/OFF Switch."

[27] Dostmann Electronic GmbH., "Precision Measuring Instruments P650, Operation Manual," Jan. 2007.